Supporting Information

Bioinspired, Highly Adhesive, Nanostructured Polymeric Coatings for Superhydrophobic Fire-Extinguishing Thermal Insulation Foam

Zhewen Ma,[⊥,†] Xiaochen Liu,[⊥,ǁ] Xiaodong Xu,[⊥,†] Lei Liu,[†] Bin Yu,[*,§] Cristian Maluk,[±] Guobo Huang,[£] Hao Wang,[‡] and Pingan Song[*,‡]

[†] *School of Engineering, Zhejiang A&F University, Hangzhou, 311300, China*

[‡] *Centre for Future Materials, University of Southern Queensland, Springfield Central, 4300, Australia*

[§] *State Key Laboratory of Fire Science, University of Science and Technology of China, Hefei 230026, China*

[±] *School of Civil Engineering, The University of Queensland Brisbane, 4072, Australia*

[£] *School of Pharmaceutical and Materials Engineering, Taizhou University, Taizhou 318000, China*

[ǁ] *College of Physics, Henan Normal University, Xinxiang 453007, China*

[*] Correspondence should be addressed:

Email: pingansong@gmail.com and pingan.song@usq.edu.au (P. Song)

Email: yubin@ustc.edu.cn (B. Yu)

[⊥] These authors contributed equally to this work.

Table of Contents

Determination of reactivity ratios. In this study, Poly (VS-co-HEA) is a binary copolymer of VS and HEA. The quantitative relationship between its instantaneous composition and monomer composition can be described by the differential equation of the following binary copolymer:

$$\frac{d[M_1]}{d[M_2]} = \frac{[M_1]}{[M_2]} \cdot \frac{r_1[M_1] + [M_2]}{r_2[M_2] + [M_1]} \qquad (1)$$

Wherein [M_1] and [M_2] represent the molar concentrations (in M) of monomers VS and HEA in the raw material system respectively; similarly, *d*[M_1] and *d*[M_2] represent the molar concentrations (in M) of monomers VS and HEA, respectively, in the transient polymerization system.

The Yezreielv Brokhina Roskin (YBR) method defines *R* as the initial ratio of molar concentration of M_1 (VS) to M_2 (HEA) and ρ as the ratio of molar concentration of M_1 (VS) to M_2 (HEA) in co-polymer at a certain instant.[1]

No.	R_i	ρ_i
1	1	0.23
2	1.22	0.32
3	1.5	0.36

Therefore, Equation 1 can be expressed as:

$$\left(\frac{R}{\rho^{1/2}}\right) \cdot r_1 - \left(\frac{\rho^{1/2}}{R}\right) \cdot r_2 + \left(\frac{1}{\rho^{1/2}} - \rho^{1/2}\right) = 0 \qquad (2)$$

By using the method of least squares, the above equation can be obtained as follows:

$$r_1 A_1 - r_2 n = C_1 \qquad (3)$$

$$-r_1 n + r_2 A_2 = C_2 \qquad (4)$$

Wherein,

$$A_1 = \sum_1^n \left(\frac{R_i^2}{\rho_i}\right) \qquad (5)$$

$$A_2 = \sum_1^n \left(\frac{\rho_i}{R_i^2}\right) \quad (6)$$

$$C_1 = \sum_1^n R_i \left(1 - \frac{1}{\rho_i}\right) \quad (7)$$

$$C_2 = \sum_1^n \frac{\rho_i}{R_i}\left(\frac{1}{\rho_i} - 1\right) \quad (8)$$

Therefore,

$$r_1 = \frac{A_2 C_1 + nC_2}{A_1 A_2 - n^2} \quad (9)$$

$$r_1 = \frac{A_1 C_2 + nC_1}{A_1 A_2 - n^2} \quad (10)$$

Using the YBR method, the reactivity ratios of VS and HEA were calculated as r1=0.20 and r2=3.96, respectively.

Characterizations. Fourier transform infrared (FTIR) spectra were recorded on a Nicolet iS50 FTIR instrument (Thermo Fisher) with a wavenumber ranging from 400 to 4000 cm^{-1}. The samples were prepared by KBr pellet pressing method. Elemental analysis (EA) measurements were conducted on a Vario EL Cube elemental analyzer. ^1H NMR spectroscopy were carried out using a Bruker-600 NMR 600 MHz spectrometer (Advance III, Bruker, Switzerland). D_2O and tetramethylsilane (TMS) were used as a solvent and an internal standard of chemical shift, respectively. The weight-average (Mw), number-average (Mn) molecular weights and PDI were obtained by a gel permeation chromatograph (GPC, PL-GPC220) eluting with H_2O.

Thermogravimetric analysis (TGA) was performed on a thermal analyzer (NETZSCH TG 209F3). Typically, approximately 3.0-8.0 mg of each specimen was heated from room temperature to 750 °C at a rate of 20 °C/min under nitrogen atmosphere at a flow rate of 100 mL min^{-1}. Each sample was tested at least 3 times. Differential scanning calorimeter (NETZSCH DSC 200F3) was used to determine the glass transition temperature (T_g) of poly(HEA-co-VS). Approximately 5.0 mg of specimen was enclosed in an aluminum pan, and nitrogen was used as the protective gas at a flow rate of 50 mL/min. Samples were heated from 0 to 65 °C at a rate of 5 °C min^{-1}, kept isothermally for 10 min prior to being

quenched to −50 °C and then heated to 250 °C at a rate of 5 °C/min. The data were obtained from the second heating scan. Each sample was tested at least 3 times.

Scanning electron microscopy (SEM) images of the poly(HEA-co-VS) surfaces were recorded on a GeminiSEM 300 (Carl Zeiss, Germany) at an accelerating voltage of 3 kV. And the SEM was coupled with an Energy Dispersive Spectrometer (EDS) microanalyzer to analyze the elemental compositions. Prior to the test, the surfaces of specimens were coated with a thin-layer gold. The morphology of as-synthesized co-polymers and their phase separation structure were also observed on a transmission electron microscopy (TEM, JEM-1200EX, Japan) at an accelerating voltage of 120 kV.

Tensile properties of as-synthesized poly(HEA-co-VS) films were measured on a TA Instruments DMAQ800 at 25 °C and 60% relative humidity. The tension rate was 2.0 mm/min and at least five specimens were tested per batch to obtain the average value. The shear adhesion strength was evaluated by using a SANS universal testing machine (CMT 6000) according to the standard ASTM F2255. The compressive strengths were also measured by a SANS universal testing machine (CMT 6000) according to ISO604-2002 and at least five specimens were tested to obtain an average value.

The reciprocating friction and wear tests were performed on a UMT-2 Universal Micro-Triboteste. A friction velocity of 50 mm/s, friction distance of 10 mm and a normal load of 1 N were applied to the specimen. All the reciprocating wear tests were carried out at room temperature and the wear rate K (cm^3/N·m) could be calculated from the mass loss by using equation :

$$K = \frac{\triangle m}{\rho LF}$$

Where Δm is the mass loss during test, ρ is the density of the specimen, L is the total sliding distance during the test and F is the applied load.

The UV aging experiment was carried out by exposing the samples to an ultraviolet lamp with a power of 20 W and an ultraviolet wavelength of 395 nm. The samples with different irradiation durations were observed microscopically.

Rheological measurements were performed on an ARES-G2 (TA Instrument, USA) with the nominal die gap of 0.45 mm, cone angle of 2° and cone diameter of 44 mm. The rheology measurement

temperature was maintained at 25 °C. The shear sweeps of samples were performed from 0.1 to 1000 s^{-1} and the frequency sweeps of samples were performed from 0.02 to 100 rad/s at a strain amplitude within the linear viscoelastic region of 5%. The contact angles of PU, FRPU and hydrophobic FRPU were recorded on a contact angle tester (TBU 100, Dataphysics, Germany).

Cone calorimetry was carried out on an FTT UK device. The combustion tests were conducted under heat fluxes of 35 kW m^{-2}, according to ASTME1354 and ISO 5660. PU specimens (100×100×30 mm^3), PLA specimens (100×100×3 mm^3), epoxy resin specimens (100×100×3 mm^3) and the wood specimens (100×100×6 mm^3) were used in this experiment. The results from the cone calorimeter tests (CCT) can be reproduced within 5% and the data reported here were averaged for triplicate experiments. Limited oxygen index (LOI) was measured on a JF-3 oxygen index meter (Jiangning, China) with specimen dimensions of 100×10×10 mm^3 according to ISO4589-2:1996. The UL-94 vertical burning test was conducted using a 5402H-V BURNING TESTER instrument and the specimen has a size of 130×13×10 mm^3 according to ASTM D 3801. Thermogravimetric analysis - infrared spectrometry (TG-IR) was carried out on the same instrument above coupled with a Fourier transform infrared (FTIR, Thermo Nicolet iS10, Thermo Scientific, Germany) spectroscope. Pyrolysis-gas chromatography-mass spectrometry (Py-GC/MS) analysis was carried out on an Agilent PY-3030D/7890B-5977A (Agilent Technologies Co. Ltd, USA). The probe was heated from room temperature to 700 ℃ at a rate of 20 °C/min and held for 10 s. X-ray diffraction (XRD) experiments were performed on a LabX XRD-6000 with Cu kα radiation. The data were recorded in the 2θ values of 5-90° at a scan speed of 3°/min with a sampling pitch of 0.02°.

All thermographic images were captured using an infrared thermal camera (FLIR E85) with a thermal sensitivity of ≤2%. Thermal conductivity was performed on a DRL-III thermal conductivity tester using 20 mW output power in the transient mode at a relative humidity of 50±10%. The sample size is 5.0×5.0×3.0 cm^3 (width×height×thickness).

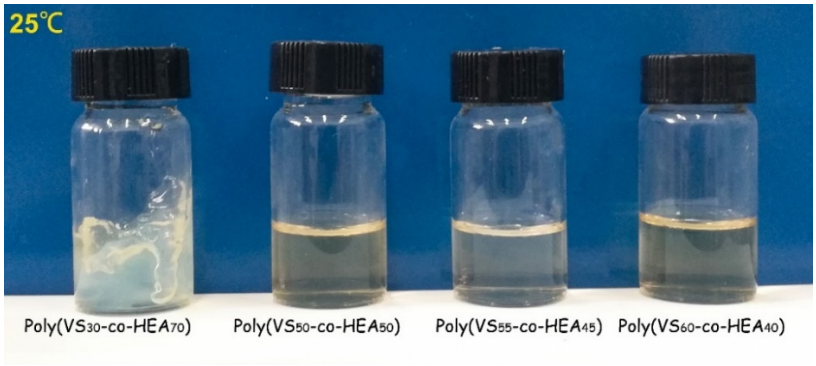

Figure S1. Digital photos of 25 wt% aqueous solutions of poly(VS-co-HEA) after polymerization (VS/HEA ratio of 70/30: incomplete polymerization; VS/ HEA ratio of 30/70: gelation).

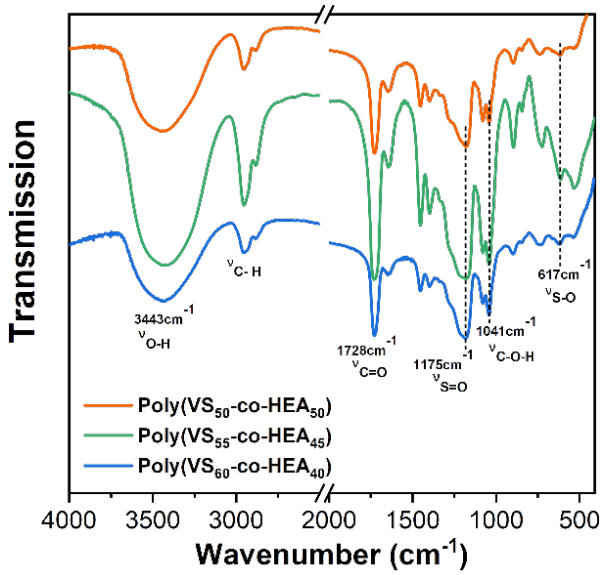

Figure S2. IR spectra of poly(VS-co-HEA) with various VS/HEA ratios.

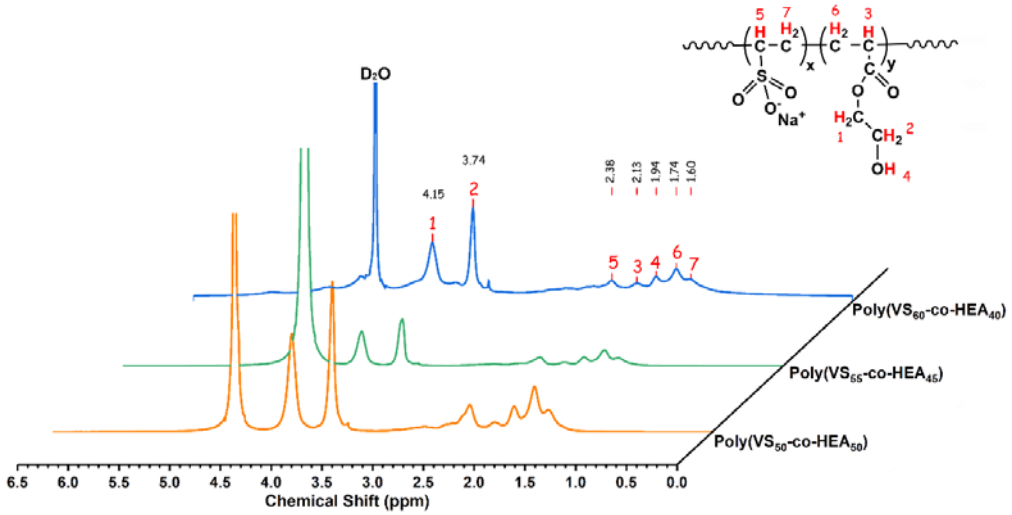

Figure S3. The ^{1}H NMR spectra of poly(VS-co-HEA) with various VS/HEA ratios.

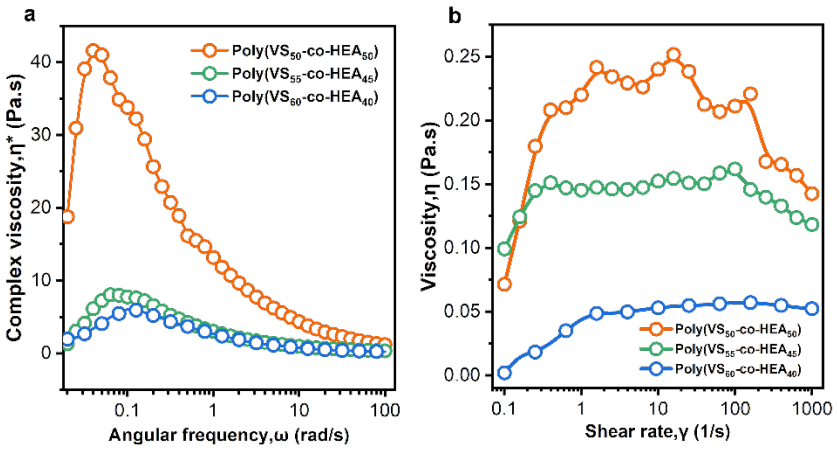

Figure S4. a) Frequency dependence of complex viscosity and b) shear rate dependence of apparent viscosity of 25 wt% aqueous solutions of poly(VS-co-HEA) with various VS/HEA ratios.

Figure S5. Digital photos of poly(VS-co-HEA) films with a VS/HEA molar ratio of a) 50/50, b) 55/45 and c) 60/40.

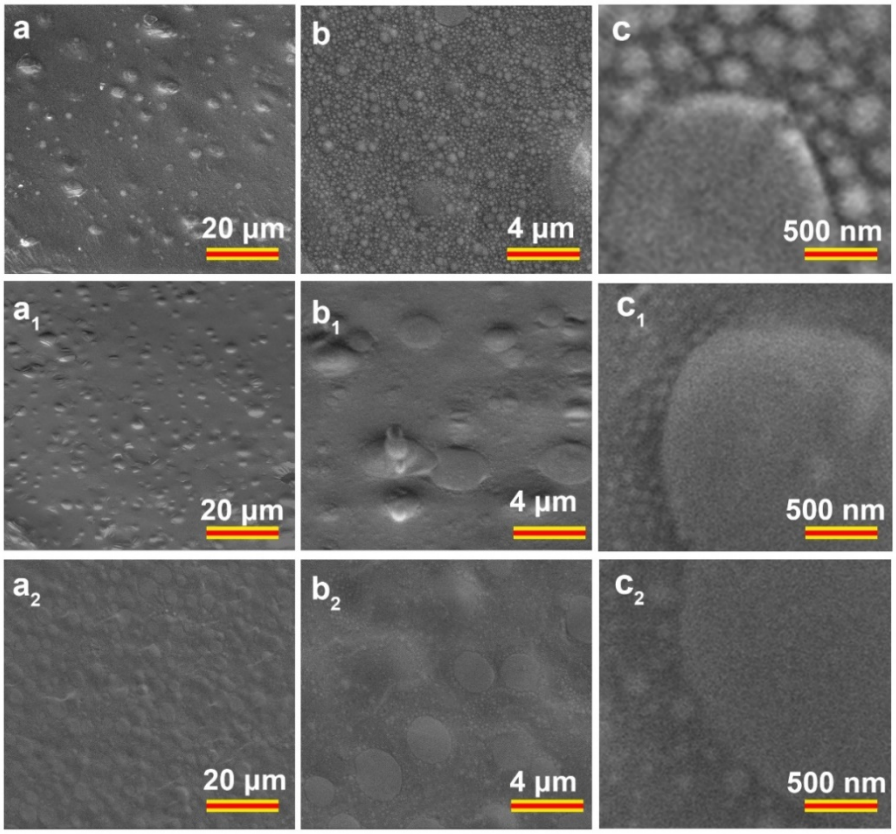

Figure S6. SEM images of poly(VS-co-HEA) films with a VS/HEA molar ratio of a,b,c) 50/50, a_1,b_1,c_1) 55/45 and a_2,b_2,c_2) 60/40.

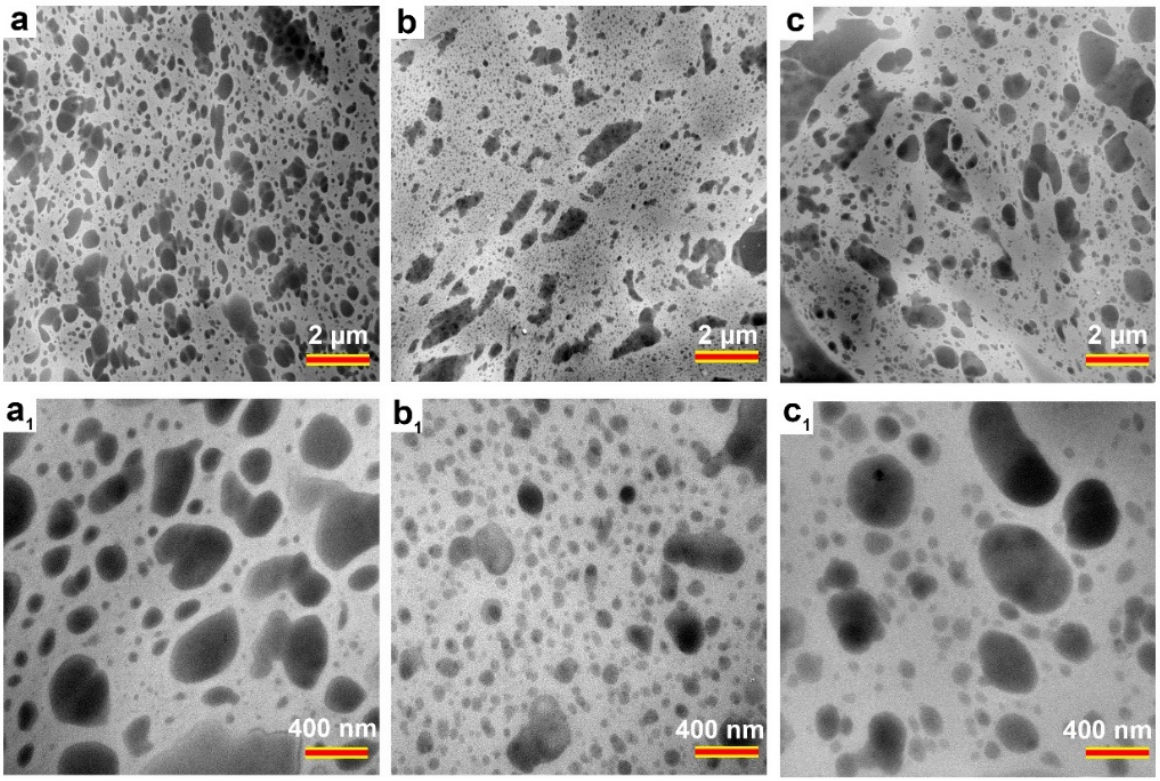

Figure S7. TEM images of poly(VS-co-HEA) films with a VS/HEA molar ratio of a,a$_1$) 50/50, b,b$_1$) 55/45 and c,c$_1$) 60/40.

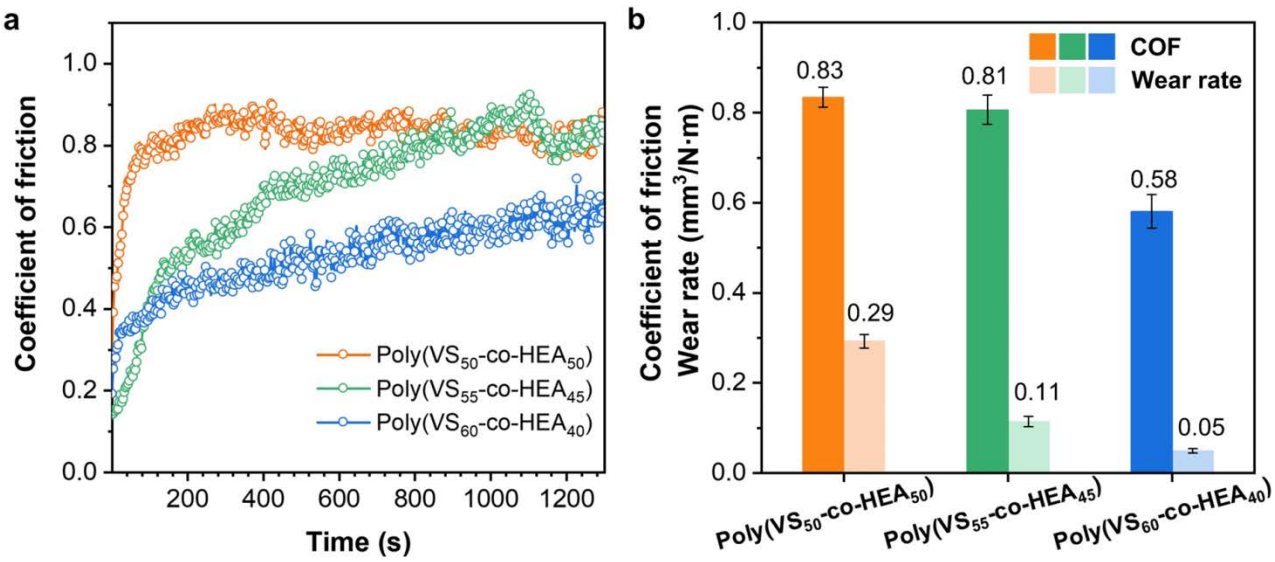

Figure S8. Friction-time curves for poly(VS-co-HEA) films with various VS/HEA ratios. a) Variation of friction coefficient with time. b) Average friction coefficient and wear rate of poly(VS-co-HEA) with different VS/HEA ratios. Overall, the poly(VS-co-HEA) shows wear resistance property to some extent, *e.g.* a coefficient of friction of 0.83 for poly(VS_{50}-co-HEA_{50}). The coefficient of friction reduces monotonously with increasing the VS/HEA ratio and a similar trend is also observed for the wear rate, indicating gradual increase in wear resistance property.

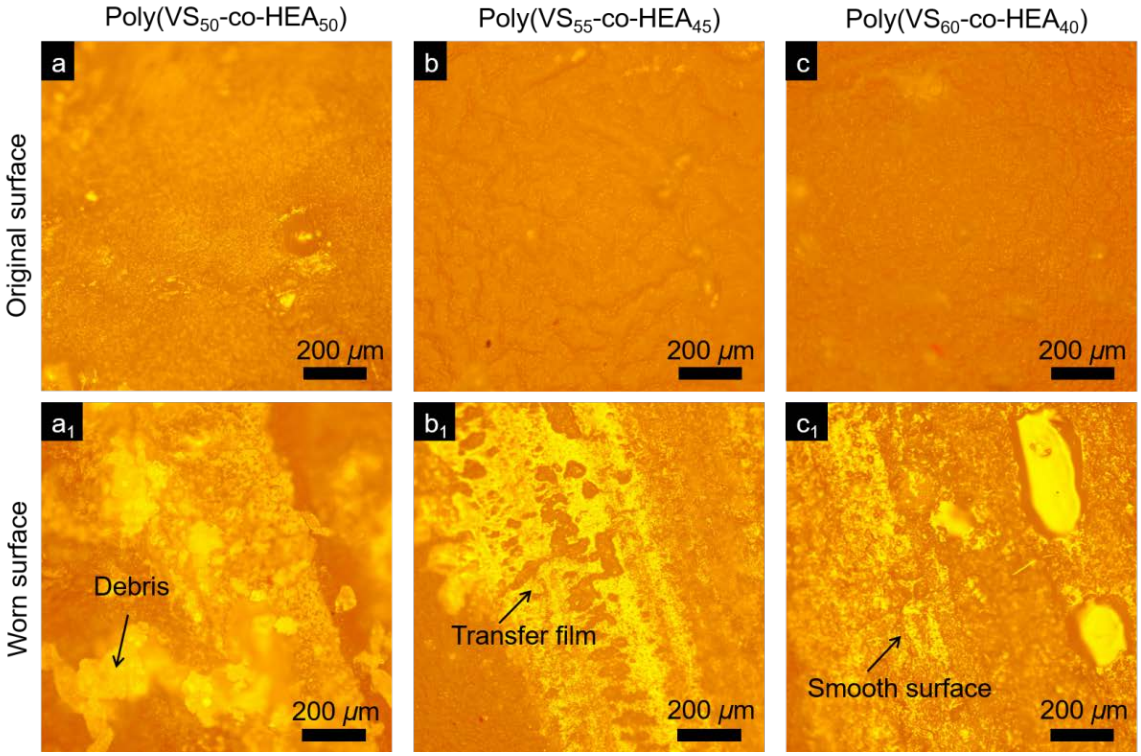

Figure S9. Optical microscopy of initial poly(VS-co-HEA) films with a VS/HEA molar ratio of a) 50/50, b) 55/45, c) 60/40 and a_1-c_1) corresponding wear track pictures of the local enlargement after reciprocating wear tests. Some debrics are observed for poly(VS_{50}-co-HEA_{50}), whereas relative smooth surface remains for poly(VS_{60}-co-HEA_{40}) after reciprocating wear tests. This result is attributed to higher rigidity of VS segments in the poly(VS-co-HEA) than HEA segments.

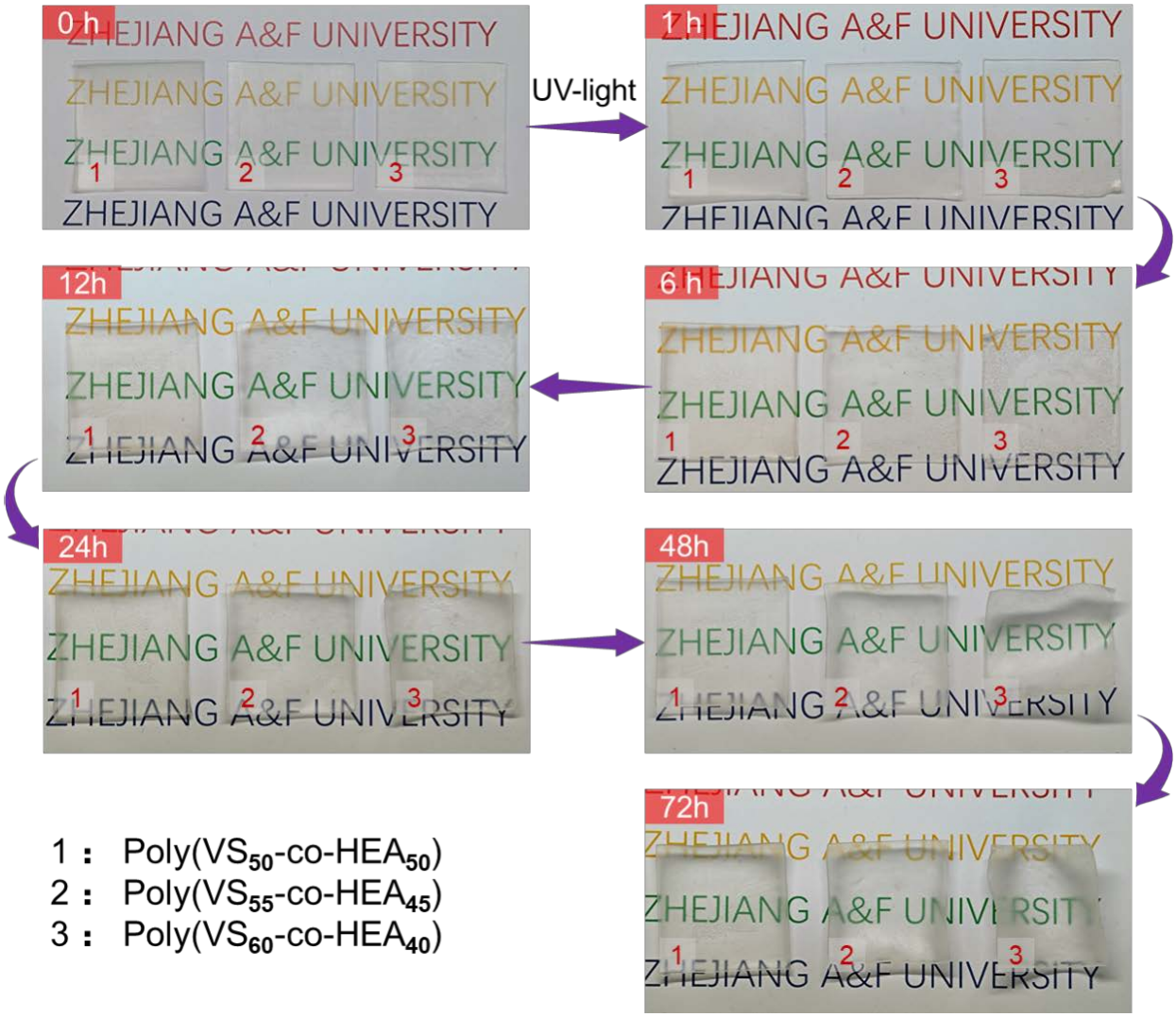

Figure S10. Digital photos of poly(VS-co-HEA) films with a VS/HEA molar ratio of 1) 50/50, 2) 55/45 and 3) 60/40 after exposure to UV light for 0-72h. After different time of UV accelerated aging, the poly(VS-co-HEA) film tend to bend and the sample with a lower VS/HEA ratio performs better in UV resistance probably due to higher contents of soft HEA segments.

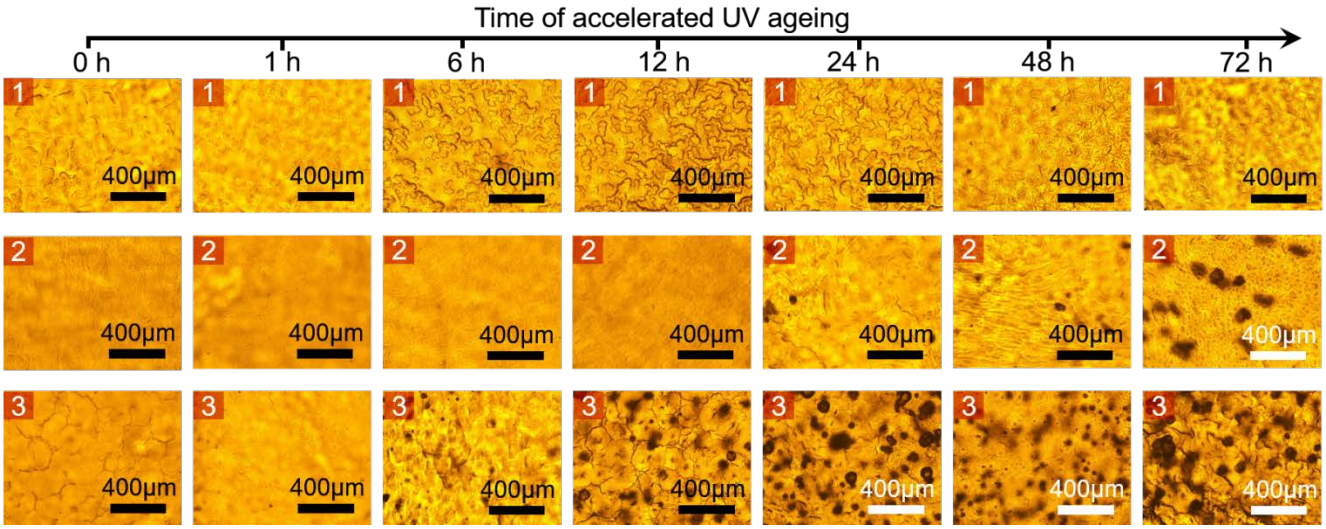

Figure S11. Optical microscopy of poly(VS-co-HEA) films after UV exposure for 0−72 h with a VS/HEA molar ratio of 1) 50/50, 2) 55/45 and 3) 60/40. There are insignificant changes observed in the morphologies of poly(VS_{50}-co-HEA_{50}) films after UV exposure for 72 h, indicating its good anti-UV ageing properties.

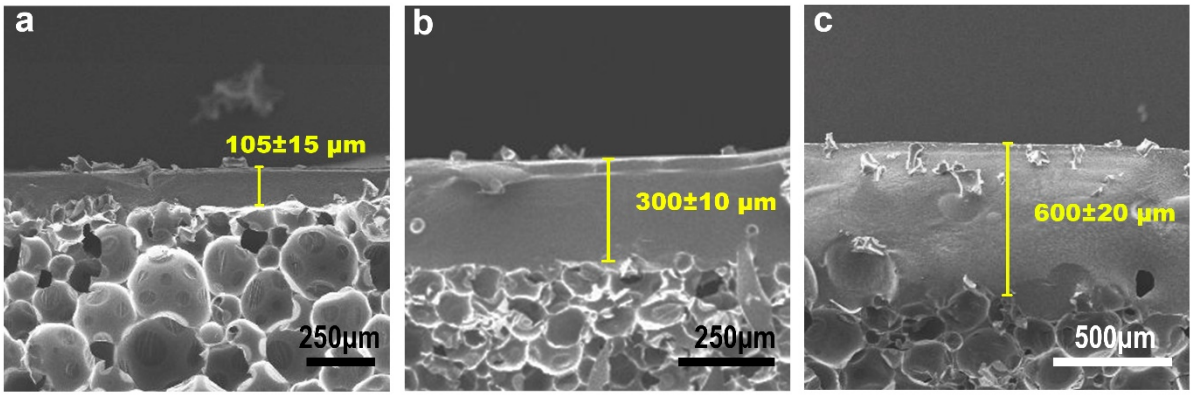

Figure S12. SEM images of FRPU with coating thickness of a) 100, b) 300 and c) 600 μm.

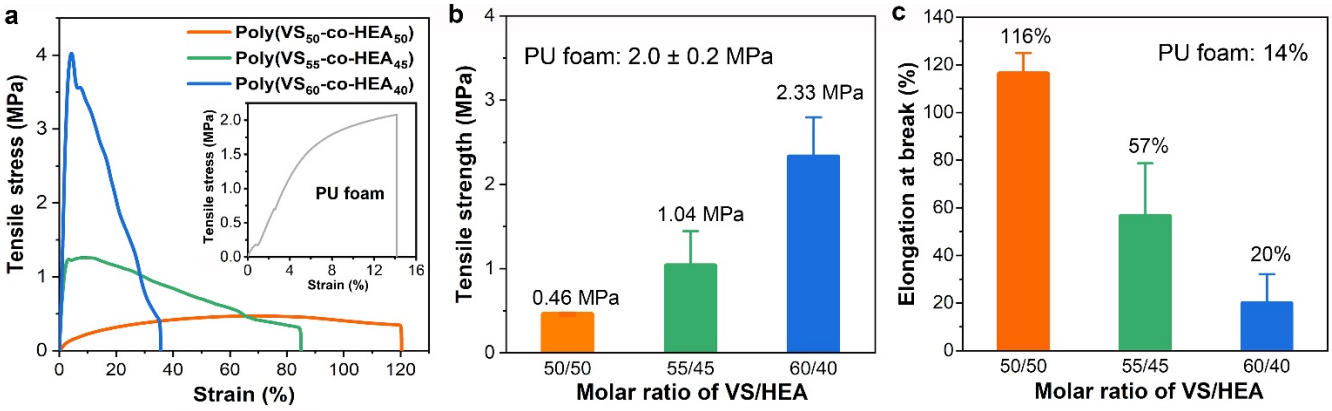

Figure S13. Mechanical properties of poly(VS-co-HEA) films. a) tensile stress-strain curves, b) tensile strength and c) elongation at break of films poly(VS-co-HEA) with various VS/HEA ratios.

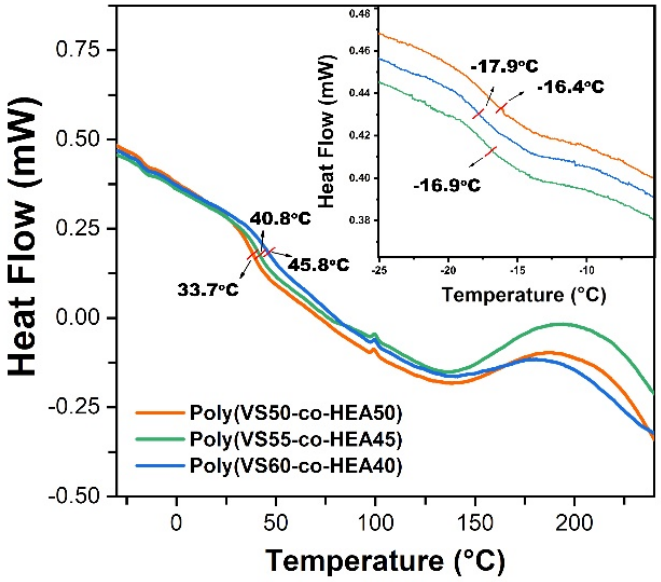

Figure S14. DSC curves of poly(VS-co-HEA) with various VS/HEA ratios.

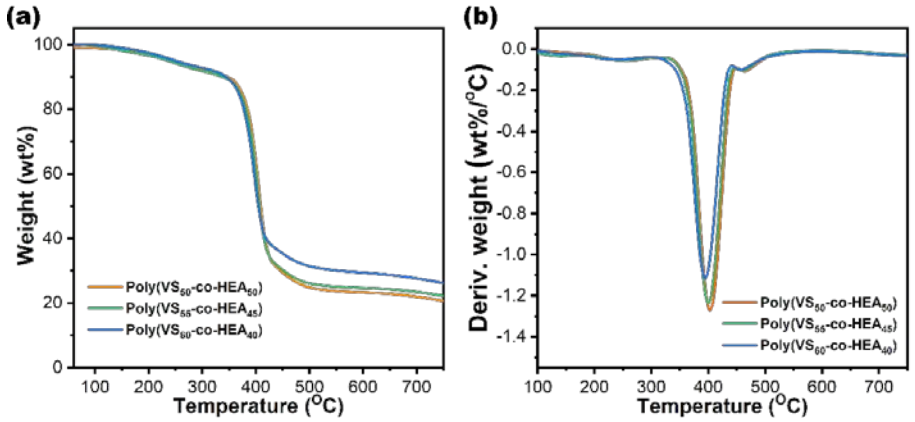

Figure S15. a) TGA and b) DTG curves of poly(VS-co-HEA) with various VS/HEA ratios in nitrogen conditions.

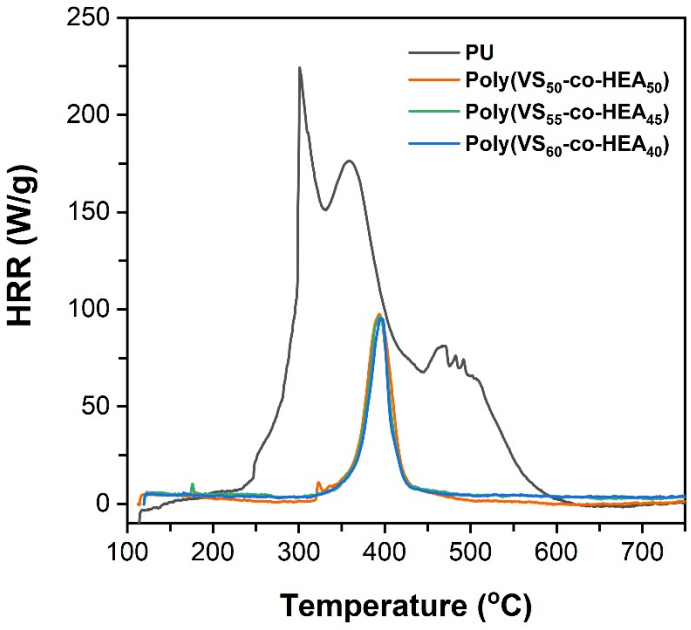

Figure S16. Heat release rate curves of pristine PU foam and poly(VS-co-HEA) with various VS/HEA ratios at a heating rate of ca. 1.0 °C/s under N_2 flow.

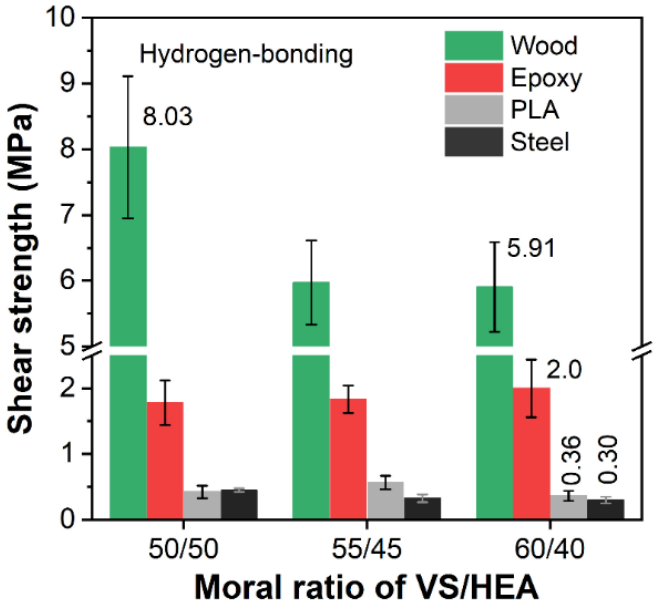

Figure S17. Shear strength of poly(VS-co-HEA) coating with various VS/HEA ratios against different substates.

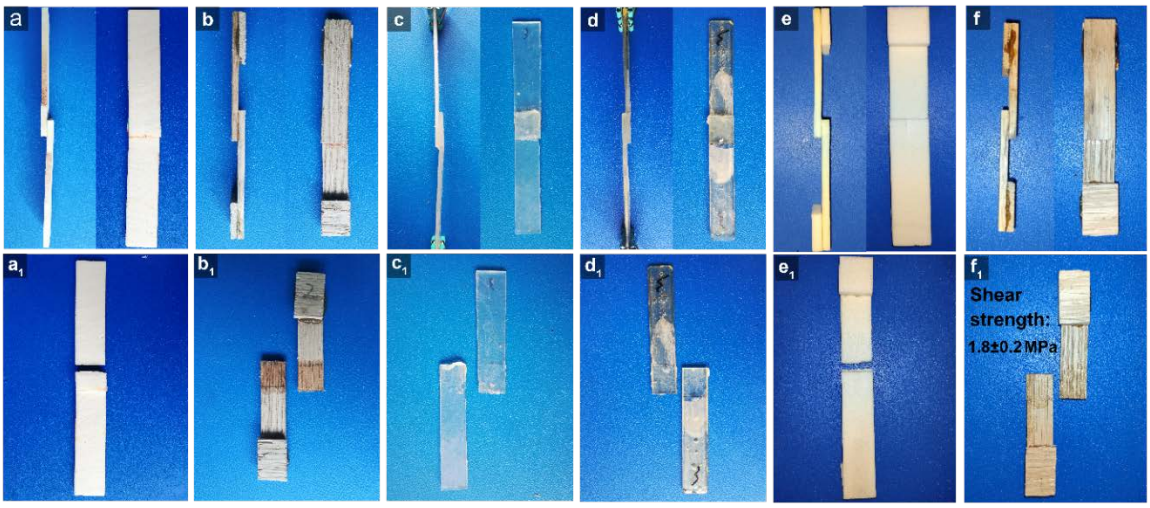

Figure S18. Digital photos of the poly(VS_{50}-c-HEA_{50}) on a, a_1) PU foams, b,b_1) wood, c,c_1)PLA and d,d_1) epoxy resin before and after adhesion tests. Digital photos of PHEA e, e_1) PU foams and f, f_1) wood after shear tests.

To assess the adhesion performance of poly(VS-co-HEA), singlelap shear tests were performed by using PU foam, PLA, wood, epoxy resin, and steel substrates. The failure mode of adhesives was determined by naked-eye visual inspection of fracture surfaces. When wood, epoxy resin and steel are used as substrates, cohesive failure occurs at the junction of the tower, both substrates surfaces are completely covered with adhesive layer after shear failure. The adhesive failure occurs when the adhesives acts on the PLA substrates, the adhesive remains covering on only one side of the substrate. However, for the PU foam substrates, all samples were broken before the adhesive failed or delaminated (Figure S14 a-d, a_1-d_1).

For comparison, the PHEA was also used as the adhesive for PU foams and wood. Likewise, the PHEA-treated PU foams also broke before the PHEA adhesive failed (Figure S14 e, e_1), indicating a high shear strength value >2.2 MPa. In comparison, the PHEA-treated wood demonstrated a shear strength of 1.8 ± 0.2 MPa, much lower than 5.91~8.03 MPa of poly(VS-co-HEA). This suggests that the poly(VS-co-HEA) has a much higher adhesion than PHEA on the wood substrate because of strong H-bonding and interfacial interlocking interactions.

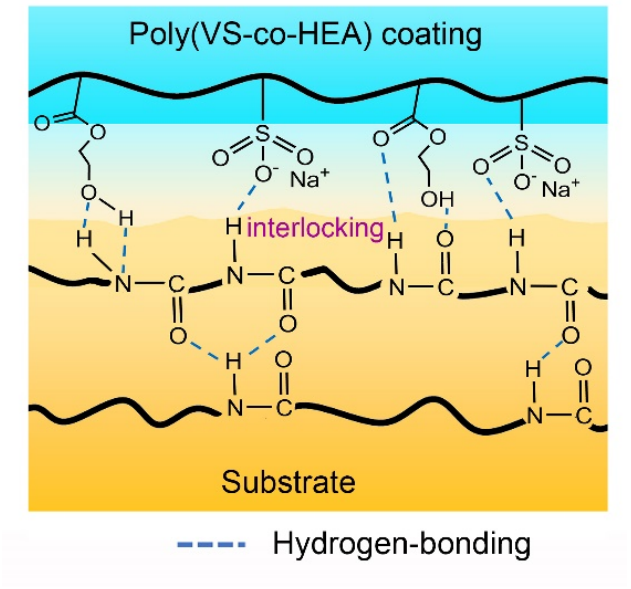

Figure S19. Schematic illustration for interfacial hydrogen-bonding between poly(VS-co-HEA) and the PU foam substrtate.

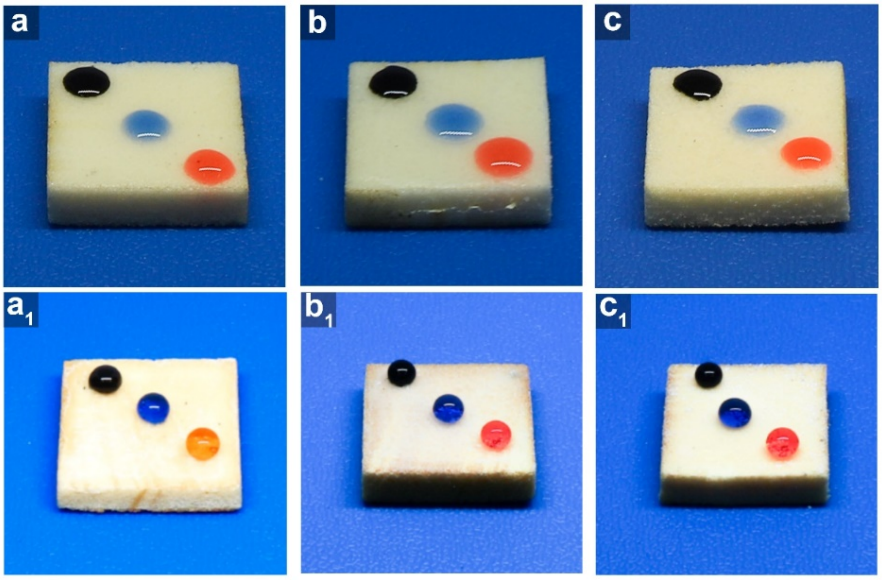

Figure S20. Digital photos of a, a1) FRPU-50/50, b, b1) FRPU-55/45 and c, c1) FRPU-60/40 before and a1, b1, c1) after hydrophobic treatment.

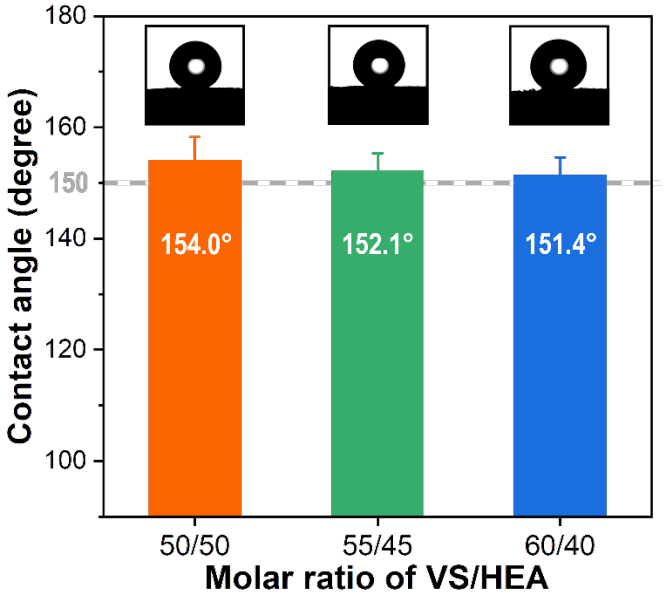

Figure S21. Contact angles of FRPU with differnt poly(VS-co-HEA) coatings with varied VS/HEA ratios. All of FRPU show a superhydrophobic feature after hydrophobic treatment.

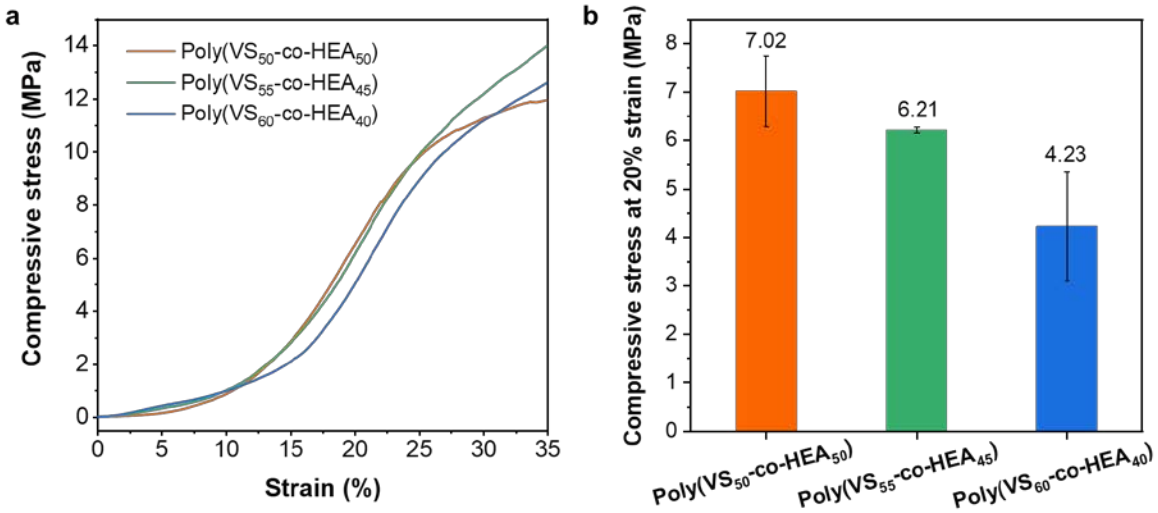

Figure S22. a) Compressive stress-strain curves and b) compressive stress of poly(VS-co-HEA) films with different VS/HEA molar ratios. The compressive strength of poly(VS-co-HEA) films gradually reduces with increasing the VS/HEA molar ratio, which agrees well with the reduction trend in the number-average molecular weight (M_n).

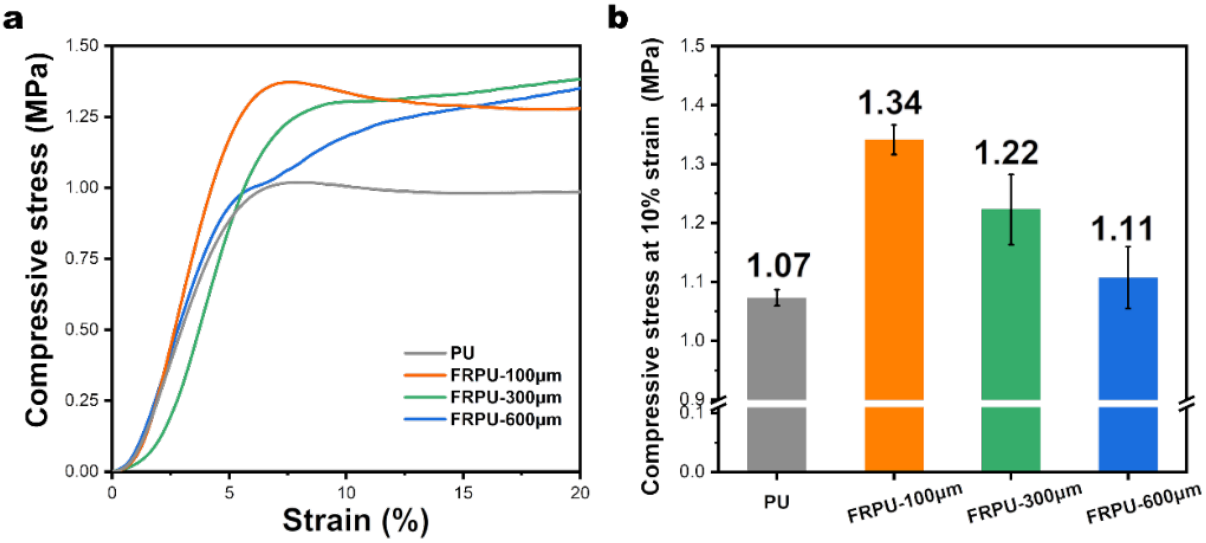

Figure S23. a) Compressive stress-strain curves and b) compressive stress of FRPU-50/50 with various coating thickness. The poly(VS-co-HEA) has advantageous impact on the compressive strength of PU foam due to its higher compressive strength than pure PU foam, in addition to strong interfacial adhesion.

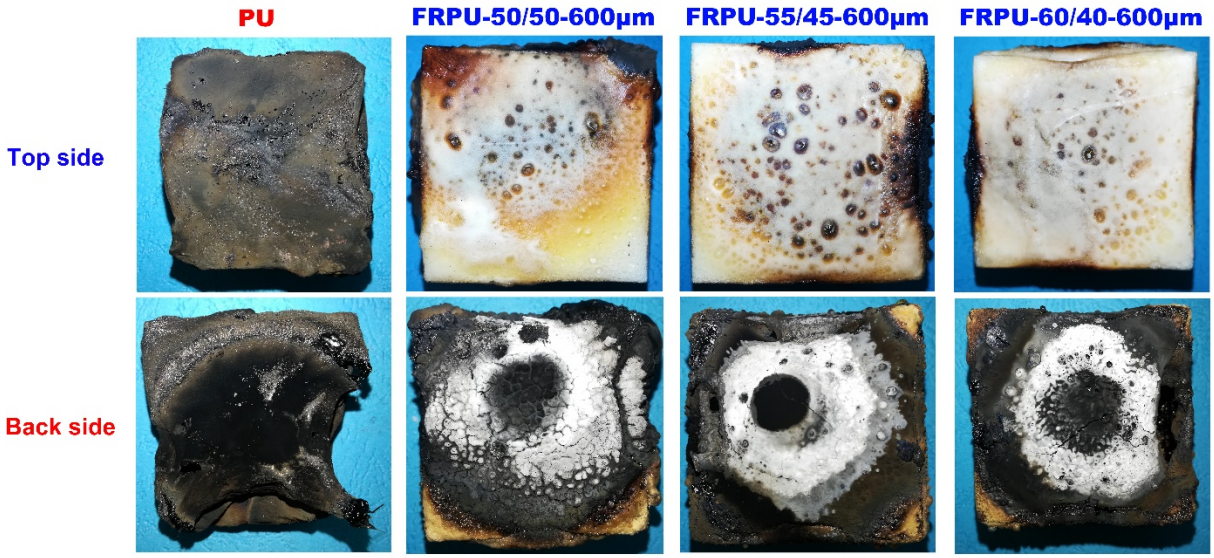

Figure S24. Digital photos of the top side and back sides of PU, FRPU-50/50-600 μ m, FRPU-55/45-600μm and FRPU-60/40-600μm before and after burning above a lamp.

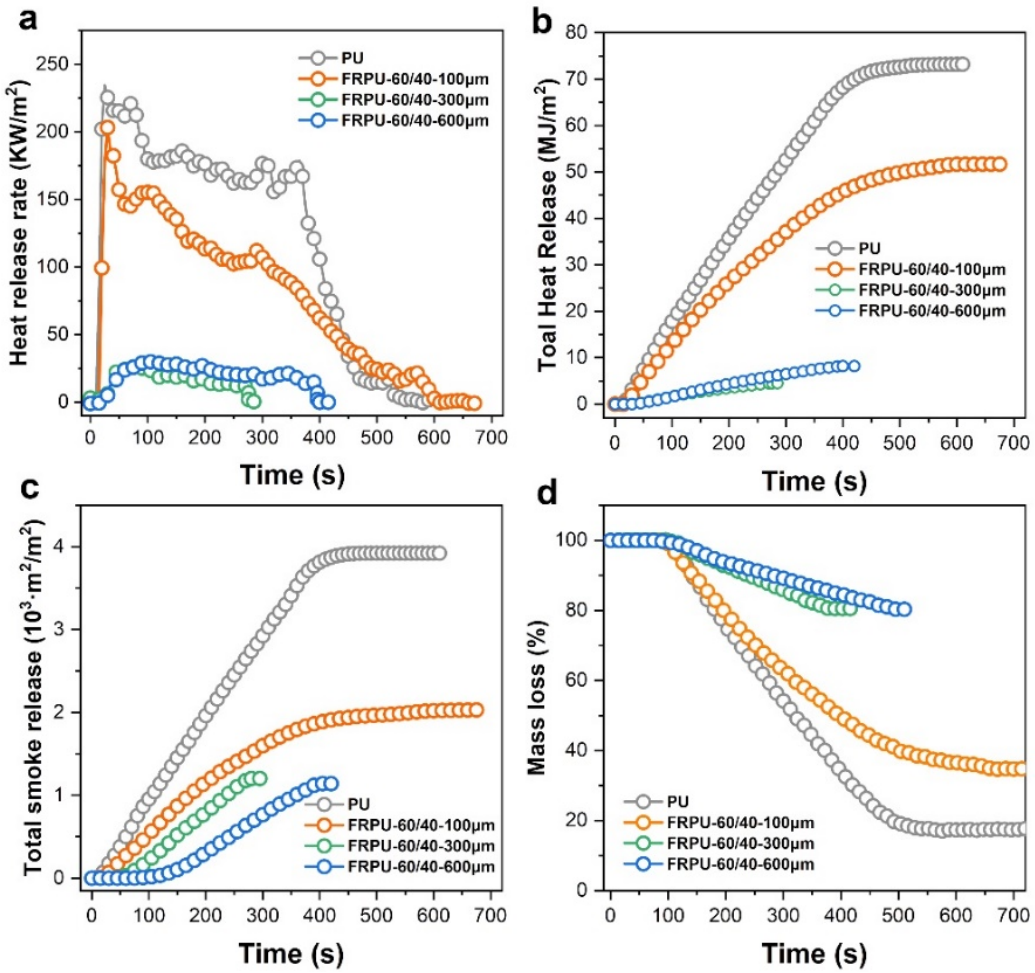

Figure S25. a) HRR, b) THR, c) TSR and d) mass loss curves of FRPU-60/40 with different coating thickness under a heat flux of 35 kW/m^2.

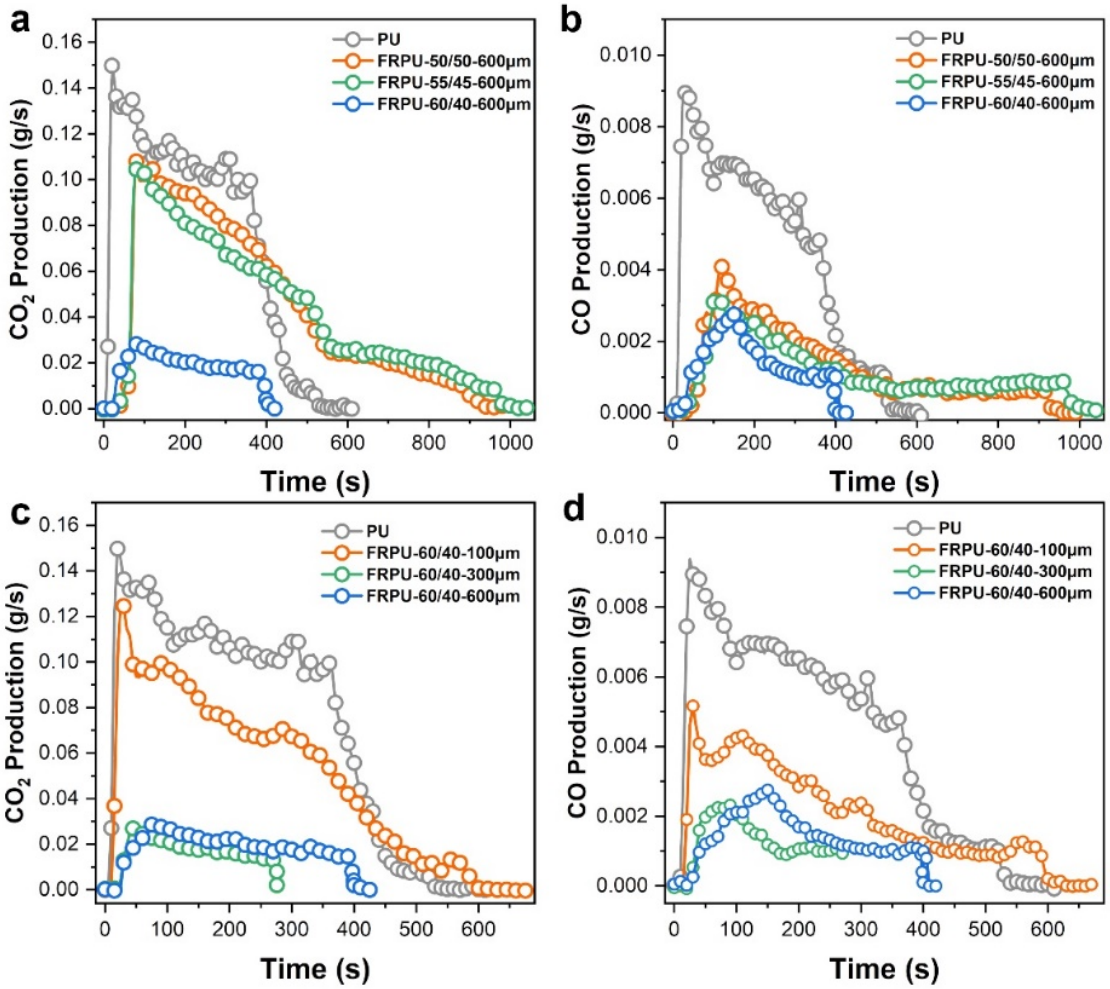

Figure S26. a) CO_2 production rate (CO_2P) and b) CO production rate (COP) curves of PU, FRPU-50/50, FRPU-55/45 and FRPU-60/40 with a coating thickness of 600 μm, c) CO_2P and d) COP curves of FRPU-60/40 with different coating thickness under a heat flux of 35 kW/m^2.

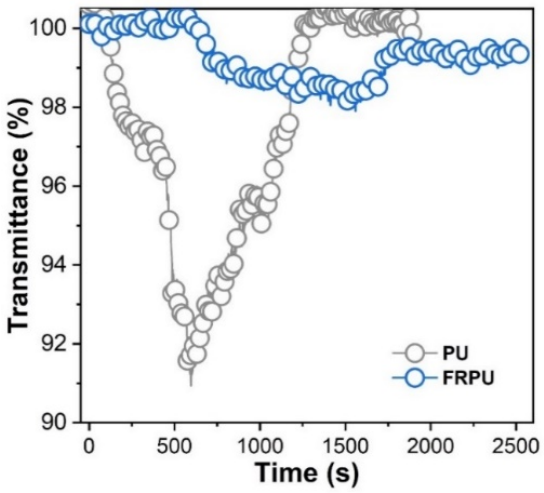

Figure S27. Smoke density curves of PU and FRPU-60/40-600μm.

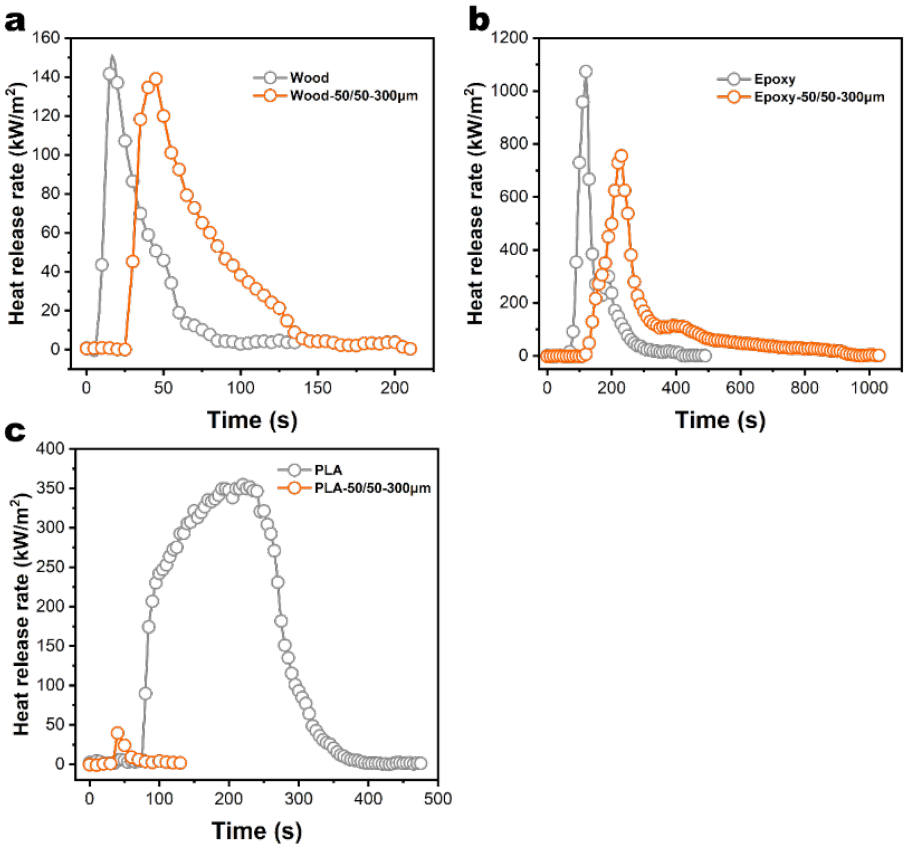

Figure S28. HRR curves of a) wood, b) epoxy resin and c) polylactic acid (PLA) before and after surface-coating treatment with 300 μm of poly(VS_{50}-co-HEA_{50}) under a heat flux of 35 kW/m^2.

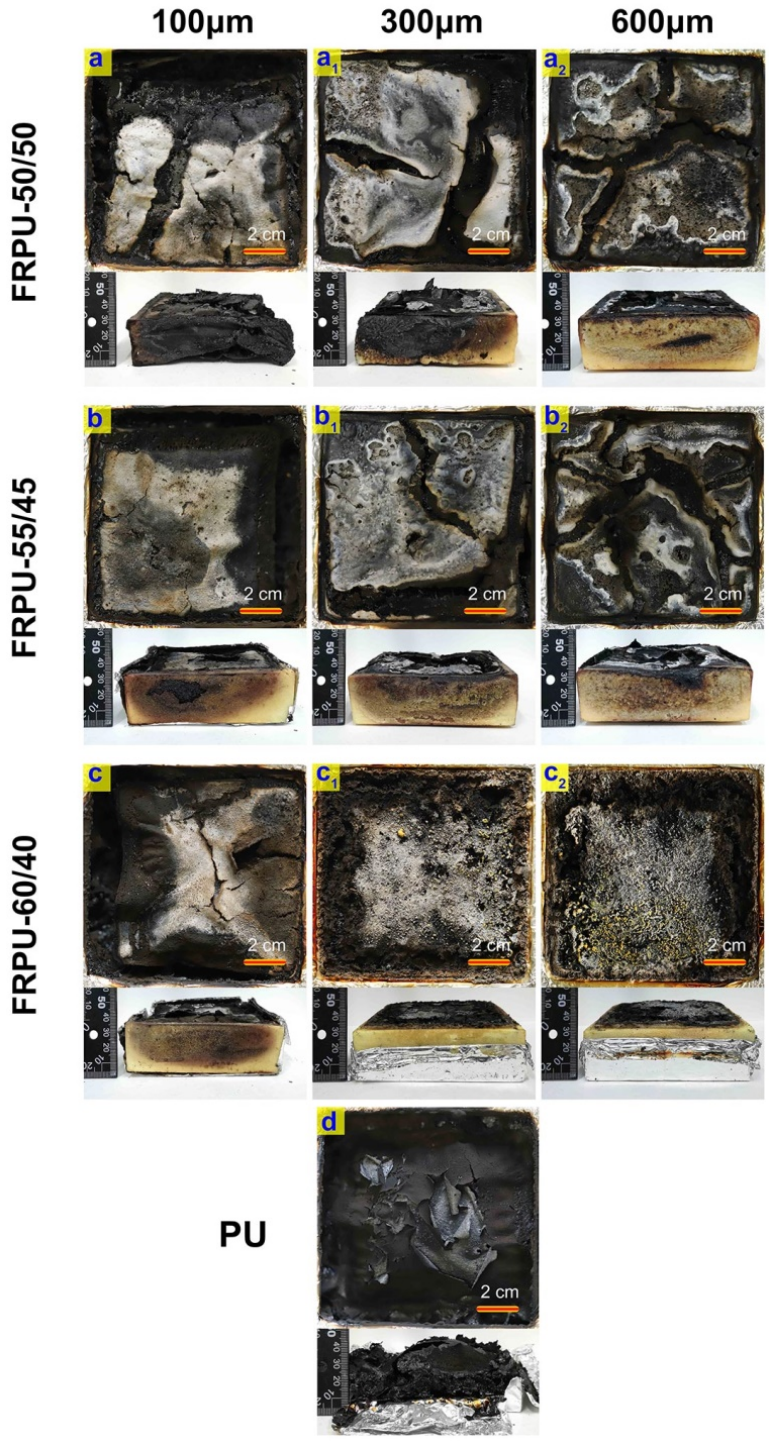

Figure S29. Digital photos of residue chars for a-a2) FRPU-50/50, b-b2) FRPU-55/45, c-c2) FRPU-60/40 and d) untreated PU after cone calorimetry tests. FRPU with a coating thickness of a-c) 100, a1-c1) 300 and a2-c2) 600 μm.

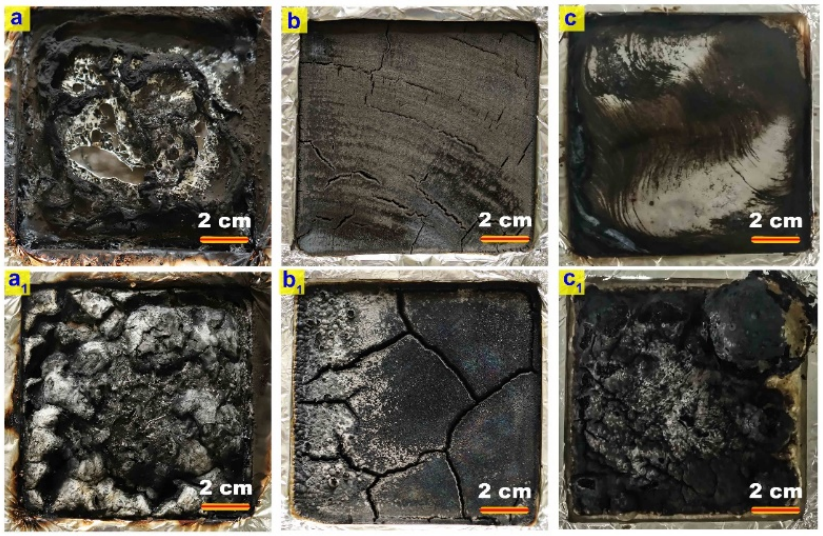

Figure S30. Digital photos of chars for a) epoxy resin, a_1) coated epoxy resin, b) wood, b_1) coated wood, c) PLA and c_1) coated PLA after cone calorimetry tests. The flame retardant coating is of 300 μm of poly(VS_{50}-co-HEA_{50}).

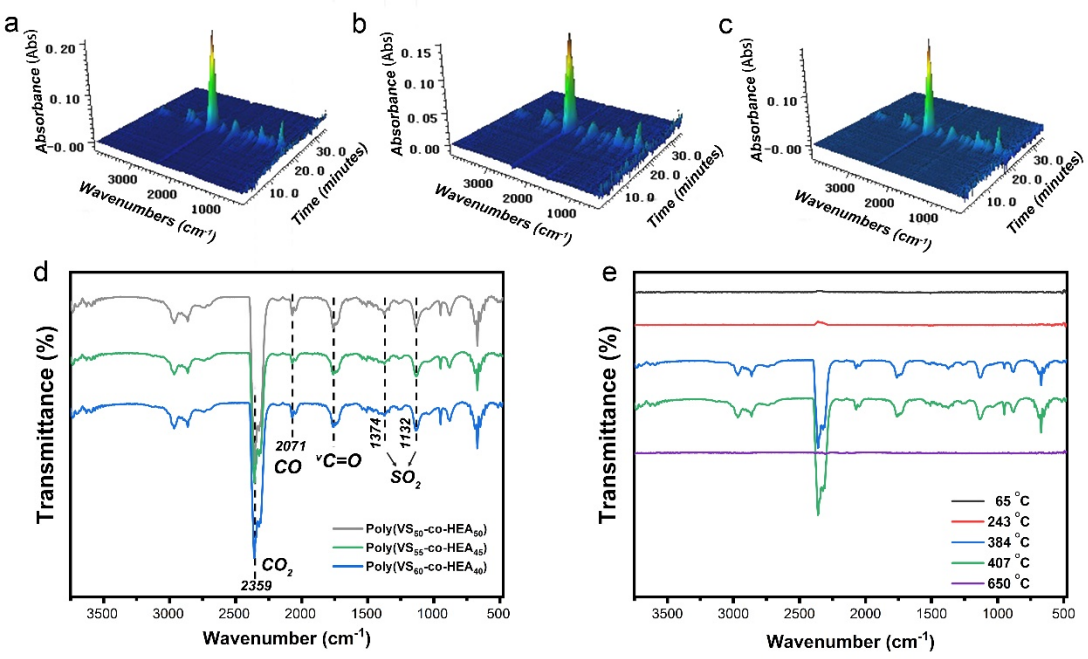

Figure S31. 3D images of TG-IR results of a) poly(VS_{50}-co-HEA_{50}), b) poly(VS_{55}-co-HEA_{45}) and c) poly(VS_{60}-co-HEA_{40}). d) IR spectra of gaseous products of poly(VS-co-HEA) with various VS/HEA ratios at T_{max} and e) poly(VS_{60}-co-HEA_{40}) at various temperatures.

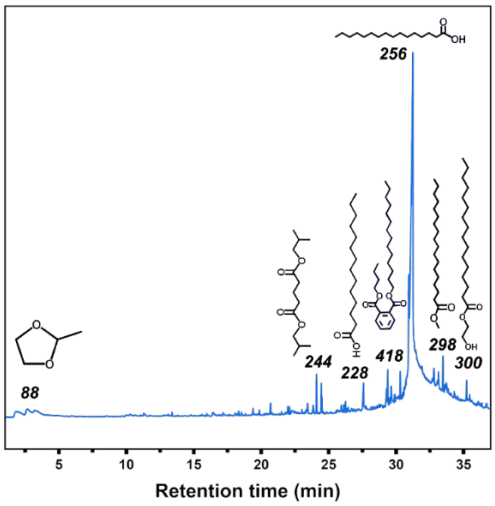

Figure S32. Gas chromatogram of the gaseous pyrolysis products for poly(VS_{60}-co-HEA_{40}).

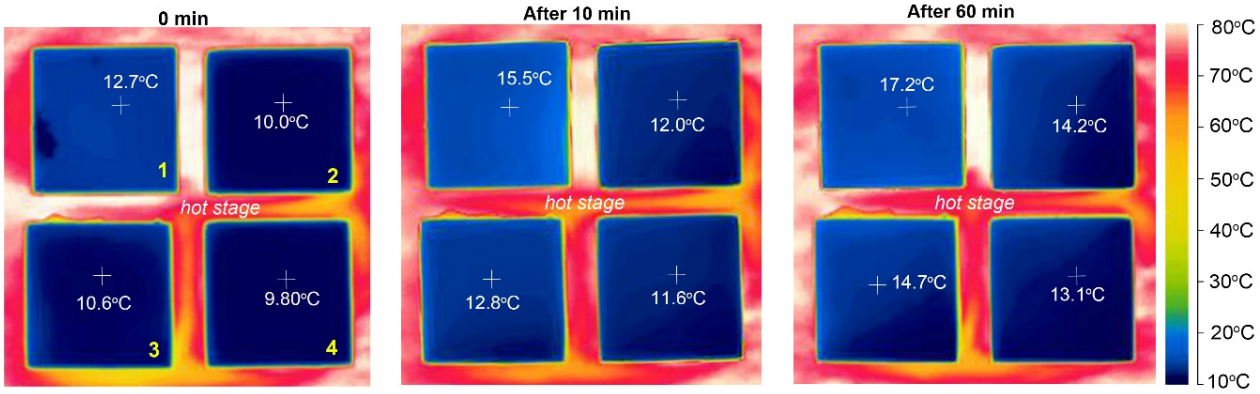

Figure S33. Digital images for the top surface temperature (TST) change with time for 1) PU, 2) FRPU-50/50-600μm, 3) FRPU-55/45-600μm and 4) FRPU-60/40-600μm on an 80 °C hot stage.

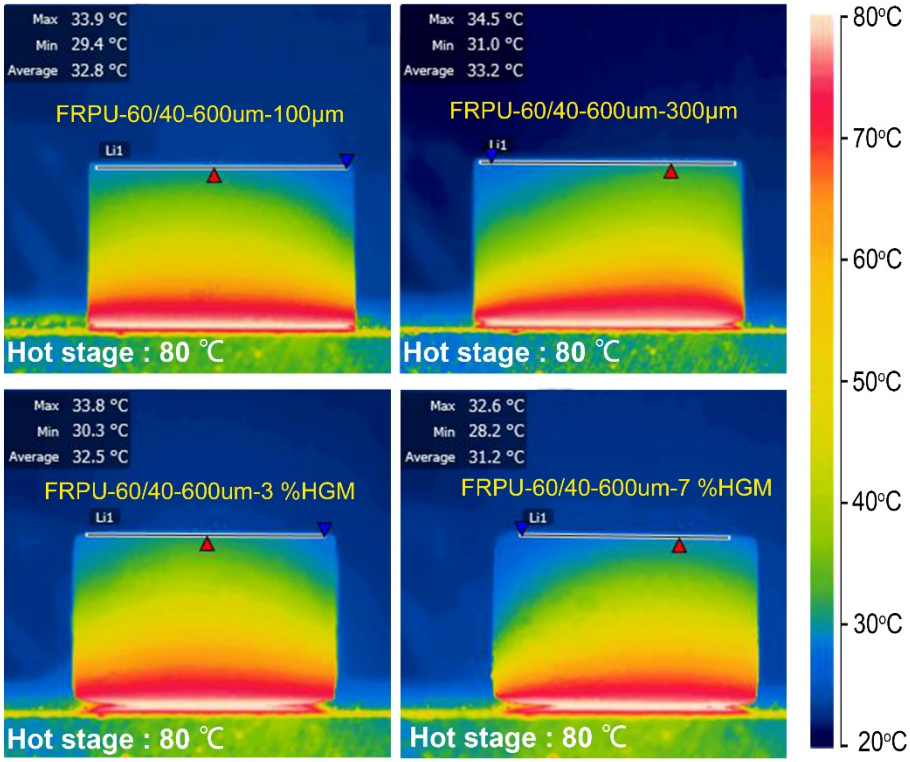

Figure S34. IR imaging of the side surface temperature for several FRPU on an 80 °C hot stage taken after 30 min.

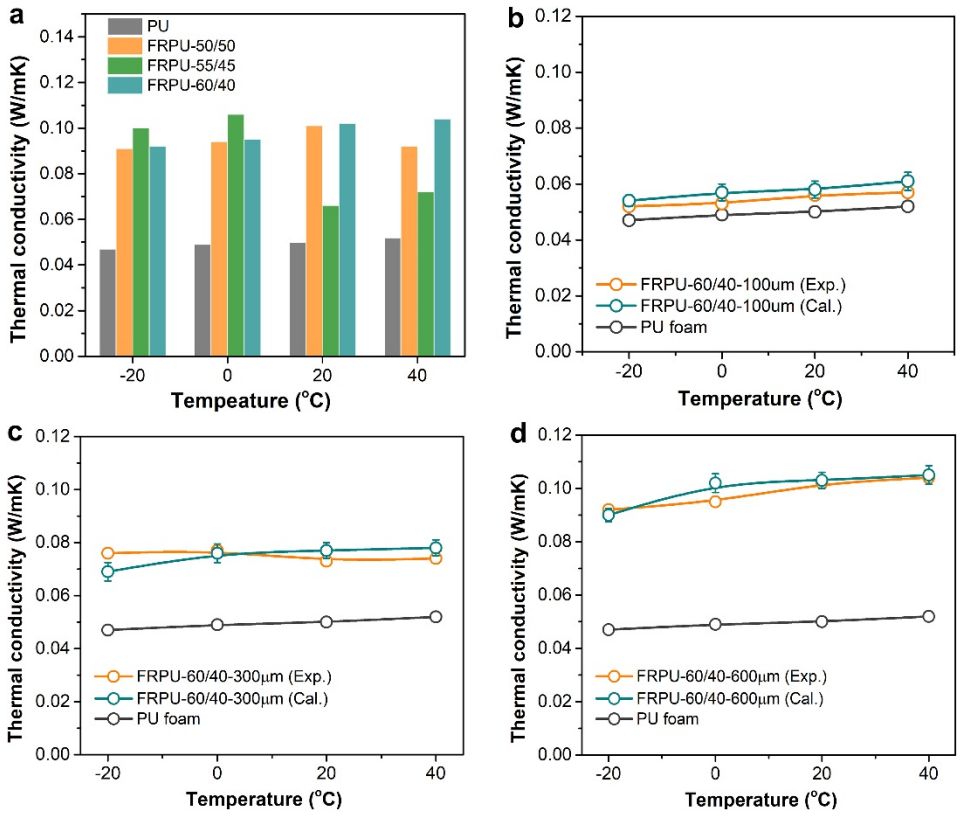

Figure S35. Temperature dependence of thermal conductivity of a) FU and FRPU with different VS/HEA ratios, b) FRPU-60/40-100μm, FRPU-60/40-300μm and d) FRPU-60/40-600μm.

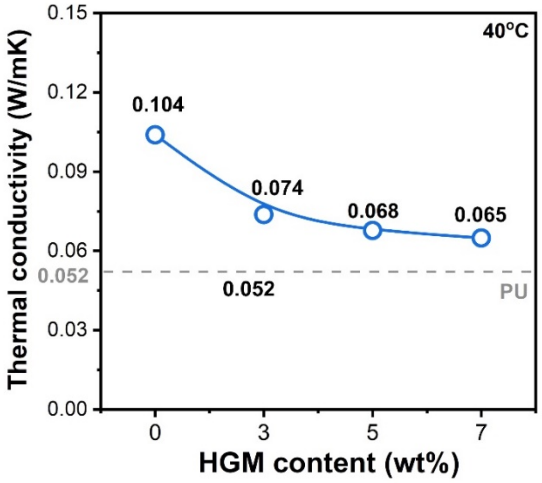

Figure S36. Thermal conductivity of FRPU-60/40-600μm containing various contents of HGM at 40 °C.

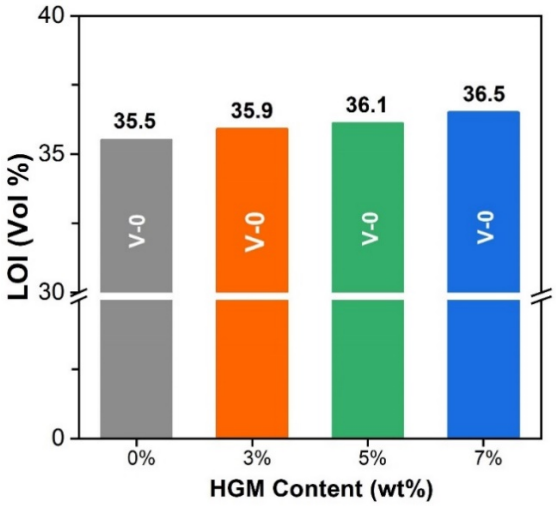

Figure S37. LOI values for FRPU-60/40-600μm containing various contents of HGM.

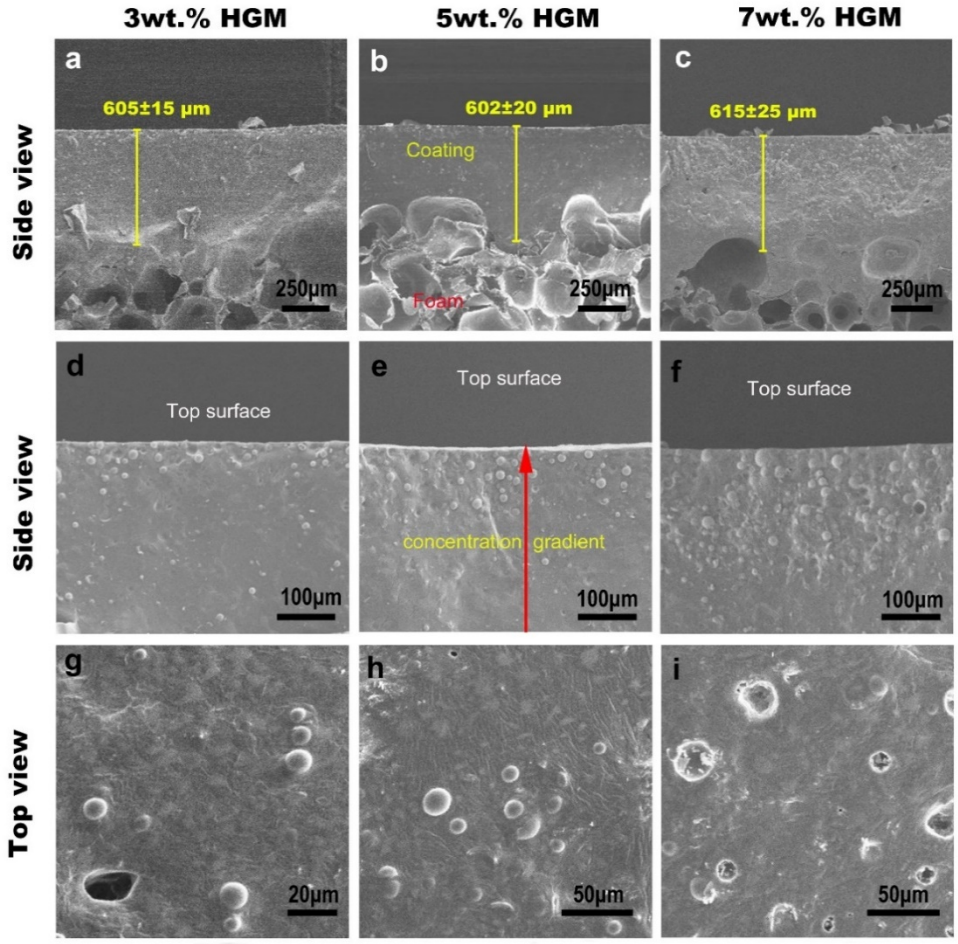

Figure S38. SEM images of FRPU-60/40 with different HGM contents, a-f) cross-section or side view and g-i) top surface.

Table S1. Elemental analysis results of poly(VS-co-HEA) with various VS/HEA ratios.

Polymer	C (wt%)	H (wt%)	O (wt%)	S (wt%)	Na (wt%)
Poly(VS_{50}-co-HEA_{50})	41.1	6.78	44.35	4.52	3.25
Poly(VS_{55}-co-HEA_{45})	37.8	6.74	45.56	5.76	4.14
Poly(VS_{60}-co-HEA_{40})	37.2	6.83	45.37	6.17	4.43

Table S2. Molecular weights, polydispersity (PDI) and densities of poly(VS-co-HEA) with various VS/HEA ratios.

Polymer	M_n (g/mol)	M_w (g/mol)	PDI	Density (g/cm^3)
Poly(VS_{50}-co-HEA_{50})	199,600	354,200	1.77	0.143
Poly(VS_{55}-co-HEA_{45})	168,700	496,650	2.94	0.145
Poly(VS_{60}-co-HEA_{40})	33,900	237,960	7.01	0.148

Table S3. Detailed thermal properties of poly(VS-co-HEA) with various VS/HEA ratios obtained from DSC and TGA measurements under nitrogen flow.

Samples	T_g [a] (°C)	T_i [a] (°C)	T_{max} [a] (°C)	Char residues at 700 °C (wt%)
Poly(VS_{50}-co-HEA_{50})	-17.9/33.7	267	403	22.0
Poly(VS_{55}-co-HEA_{45})	-16.9/40.8	245	401	23.4
Poly(VS_{60}-co-HEA_{40})	-16.4/45.8	237	394	27.6

[a] T_g, T_i and T_{max} refer to the glass transition temperature, the initial thermal degradation temperature where 5wt% weight loss occurs, and the maximum weight loss temperature, respectively.

Table S4. Flame retardancy performances of PU foam and poly(VS-co-HEA) copolymers with various VS/HEA ratios.

Sample	LOI (vol%)	UL-94 rating	T_{PHRR} [a] (°C)	THR a (kJ/g)	PHRR [a] (W/g)	HRC [a] (J/g·K)
Poly(VS_{50}-co-HEA_{50})	33.2	V-0	394	5.1	97.6	98.7
Poly(VS_{55}-co-HEA_{45})	35.5	V-0	393	5.0	96.3	98.3
Poly(VS_{60}-co-HEA_{40})	35.7	V-0	396	4.5	95.1	97.1
PU	18.8	NR	301	32.7	234	239

[a] T_{PHRR}, THR, PHRR and HRC refer to the temperature where the peak heat release rate occurs, total heat release, peak heat release rate, and heat release capacity, respectively.

Table S5. Detailed flame-retardant parameters of PU foams, epoxy, wood and PLA before and after flame-retardant surface treatment.

Run	Mass (g)	UL-94 ratings	LOI (vol%)	t_{ign} （s）	PHRR (kW/m^2) ）	THR (MJ/m^2) ）	TSR (m^2/m^2) ）	t_{PHRR} (s)	Char (wt%)）	FGI (kW/m^2•s)	FPI (m^2•s/kW)
PU	44.8	NR	18.8	13	235	73.2	3912	25	17.5	9.39	0.06
FRPU-50/50-100μm	46.26 (+10.7%)	NR	26.9	16	241	70.7	2535	25	25.3	9.63	0.07
FRPU-50/50-300μm	60.55 (+34.4%)	V-1	32.5	44	226	65.3	2293	60	41.8	3.76	0.20
FRPU-50/50-600μm	72.03 (+59.0%)	V-0	32.8	68	164	66.6	2262	120	48.2	1.37	0.41
FRPU-55/45-100μm	45.26 (+11.9%)	NR	29.0	21	219	59.3	2338	35	32.7	6.26	0.10
FRPU-55/45-300μm	59.65 (+33.5%)	V-1	33.1	37	185	63.8	2103	70	41.9	2.64	0.20
FRPU-55/45-600μm	73.44 (+69.1%)	V-0	35.2	67	171	65.2	1804	100	50.0	1.71	0.39
FRPU-60/40-100μm	42.27 (+13.1%)	NR	29.2	16	203	51.7	2025	30	34.9	6.78	0.08
FRPU-60/40-300μm	60.72 (+35.0%)	V-1	33.8	30	26.1	4.45	1203	75	80.4	0.35	1.19
FRPU-60/40-600μm	75.58 (+72.5%)	V-0	35.5	31	30.9	8.21	1142	115	80.6	0.27	0.94
FRPU-60/40-600μm-3%HGM	76.07 (+72.1%)	V-0	35.9	48							
FRPU-60/40-600μm -5%HGM	75.17 (+64.8%)	V-0	36.1	62							
FRPU-60/40-600μm -7%HGM	77.77 (+64.8%)	V-0	36.5	50							
Epoxy resins	30.88			59	1074.61	68.22	3082.37	120	11.08	8.96	0.05
Epoxy-50/50-300μm	55.96 (+81.2%)			111	755.77	104.31	4365.15	230	18.69	3.29	0.15
Wood	23.35			9	141.66	4.40	11.91	15	85.86	9.44	0.06
Wood-50/50-300μm	35.20 (+50.7%)			29	139.06	7.12	12.79	45	79.90	3.09	0.21
PLA	33.9			77	354.71	65.17	7.75	220	2.27	1.61	0.22
PLA-50/50-300μm	46.60 (+37.5%)			36	39.65	0.92	1.21	40	94.49	0.99	0.91

Table S6. The use amount of flame retardant coating for PU, epoxy, wood and PLA.

	PU	FRPU-50/50-100μm	FRPU-50/50-300μm	FRPU-50/50-600μm	FRPU-55/45-100μm	FRPU-55/45-300μm	FRPU-55/45-600μm	FRPU-60/40-100μm	FRPU-60/40-300μm	FRPU-60/40-600μm
Adhesive applied (kg/m^2)	0	0.14	0.48	0.83	0.15	0.47	0.93	0.14	0.48	0.95

	FRPU-60/40-600μm-3%HGM	FRPU-60/40-600μm - 5%HGM	FRPU-60/40-600μm - 7%HGM	Epoxy-50/50-300μm	Wood-50/50-300μm	PLA-50/50-300μm
Adhesive applied (kg/m^2)	0.99	0.92	0.95	1.12	0.42	0.60

Table S7. Elemental composition of the residual char for PU and FRPU-60/40-600 μ m after cone calorimetry tests.

	C (wt%)	N (wt%)	O (wt%)	S (wt%)	Na (wt%)	Si (wt%)	F (wt%)
PU	71.69	10.30	18.01	0	0	0	0
FRPU-60/40	7.92	0	37.23	24.41	28.80	1.44	0.2

Table S8. Thermal conductivity of PU, poly(VS-co-HEA) coating and FRPU.

Run	Thermal conductivity (W/mK)					
	- 40 °C	-20 °C	0 °C	20 °C	40 °C	60 °C
PU	0.038	0.047	0.049	0.050	0.052	0.059
poly(VS_{60}-co-HEA_{40})		0.381	0.468	0.465	0.466	
FRPU-50/50-100μm		0.055	0.056	0.055	0.057	
FRPU-50/50-300μm		0.071	0.072	0.069	0.069	
FRPU-50/50-600μm		0.091	0.094	0.101	0.092	
FRPU-55/45-100μm		0.053	0.055	0.056	0.056	
FRPU-55/45-300μm		0.079	0.082	0.076	0.082	
FRPU-55/45-600μm		0.100	0.106	0.066	0.072	
FRPU-60/40-100μm		0.052 (0.054)	0.053 (0.057)	0.056 (0.058)	0.057 (0.061)	
FRPU-60/40-300μm		0.076 (0.069)	0.077 (0.076)	0.073 (0.077)	0.074 (0.078)	
FRPU-60/40-600μm		0.092 (0.090)	0.095 (0.102)	0.102 (0.103)	0.104 (0.105)	
FRPU-3%HGM (9.0 vol %)					0.074 (0.081)	
FRPU-5%HGM (14.4 vol %)	0.048	0.055 (0.067)	0.058 (0.078)	0.061 (0.080)	0.068 (0.081)	0.071
FRPU-7%HGM (19.4 vol %)					0.065 (0.078)	
HGM (0.36g/cm^3)				0.050		

The values in the bracelet are the theoretical values according to the thermal conductivity (λ) of PU, poly(VS_{60}-co-HEA_{40}) and HGM at different temperatures, assuming the λ of HGM remains a constant from -20 to 40 °C. The values in the bracelet are calculated.

Movies S1-S2

Movie S1: Flammability tests of PU and FRPU with different poly(VS-co-HEA) by using an alcohol lamp.

Movie S2: UL-94 tests of PU and FRPU with different poly(VS-co-HEA).

REFERENCES

[1] Yezrielev, A. I.; Brokhina, E. L.; Roskin, Ye. S. An Analytical Method for Calculating Reactivity Ratios. *Polym. Sci. U.S.S. R.*, **1969**, *11* (8), 1894-1907.